Talanta 79 (2009) 1233–1237

Contents lists available at ScienceDirect

Talanta

journal homepage: www.elsevier.com/locate/talanta

Nanocomposite based on depositing platinum nanostructure onto carbon nanotubes through a one-pot, facile synthesis method for amperometric sensing

Dan Wen[a,b], Xiangqin Zou[a,b], Ying Liu[a,b], Li Shang[a,b], Shaojun Dong[a,b,*]

[a] State Key Laboratory of Electroanalytical Chemistry, Changchun Institute of Applied Chemistry, Chinese Academy of Sciences, Changchun, Jilin 130022, PR China
[b] Graduate School of the Chinese Academy of Sciences, Beijing 100039, PR China

ARTICLE INFO

Article history:
Received 16 February 2009
Received in revised form 5 May 2009
Accepted 7 May 2009
Available online 22 May 2009

Keywords:
Nanocomposite
Carbon nanotubes
Electrocatalysis
Biosensor
Enzyme

ABSTRACT

Platinum nanoparticles (Pt NPs) were deposited onto multi-walled carbon nanotubes (MWNTs) through direct chemical reduction without any other stabilizing agents. Transmission electron microscopy (TEM), X-ray photoelectron spectroscopy (XPS) and cyclic voltammetry were employed to characterize the morphology of the as-prepared nanocomposite (noted as Pt NPs–MWNTs) and further identify the Pt NPs on the surface of MWNTs. The nanocomposite demonstrated the ability to electrocatalyze the oxidation of hydrogen peroxide and substantially raises the response current. A sensitivity of 591.33 μA mM^{-1} cm^{-2} was obtained at Pt NPs–MWNTs modified electrode. Thus, we immobilized glucose oxidase (GOD) as a model enzyme on the nanocomposite-based electrode with a thin layer of Nafion to fabricate a glucose biosensor, which showed sensitive and fast response to glucose. The influence of the GOD loading was investigated and the biosensor with an enzyme loading concentration of 10 mg/mL shows optimal performance for glucose detection, that is, a detection limit of 3 μM and a response time of 3 s, respectively.

1. Introduction

Platinum (Pt) is one of the mostly researched noble metals as its potential applications have been demonstrated in the fields of biosensors, catalysts and fuel cells [1–3]. Due to its good performance toward the detection of hydrogen peroxide (H_2O_2), a typical enzymatic product, Pt, in the form of Pt electrode and Pt nanostructures modified electrodes, has been widely used to immobilize enzyme for the fabrication of glucose biosensors [4–6]. The Pt nanostructures modified substrates give high sensitivity and good selectively for H_2O_2 sensing owing to their extraordinary catalytic properties over bulk metal [7]. Pt nanoparticles (Pt NPs), which have been reported to be very effective as a matrix for enzyme sensors by taking advantages of its biocompatibility, large surfaces area and good electrocatalytic activity toward H_2O_2 [8].

Carbon nanotubes (CNTs) have been proposed as the efficient metal catalyst support for electocatalytic and sensing applications because of their unique electrical properties, high chemical stability, and high surface-to-volume ratios [9–12]. Considering the excellent electrochemical characteristic of both CNTs and Pt NPs, electrode materials combining these two would be ideal for biosensing application, and some promising results have been reported. Hrapovic et al. improved sensing performance by using CNTs network along with Pt NPs as the electrode materials [13,14]. Shen and co-workers fabricated a type of Pt NPs-doped sol–gel multi-walled carbon nanotubes (MWNTs) composite for glucose sensing which permitted low potential detection with an improved sensitivity [15]. Recently, a sensitive cholesterol biosensor based on CNTs–chitosan–Pt NPs nanocomposite was reported [16].

However, methods developed to decorate carbon nanotubes with metal nanoparticles typically involve harsh oxidative pretreatment and/or modification with surfactants or other stabilizing agents making them less useful in potential applications [17–19]. It has been reported the spontaneous nucleation of bare Pt and Au nanoparticles on CNTs side walls, however, the nanotubes themselves are oxidatively consumed in the process [20,21]. Electrodeposition of Pt NPs on CNTs is a very common way to prepare Pt NPs/CNTs nanocomposite used in sensing application. In the present work, a new, one-pot preparation procedure has been developed, which reduced the preparation complexity, since the growth of Pt NPs and the synthesis of Pt NPs–MWNTs nanocomposite were carried out in the same pot. What was more, neither stabilizing agents nor rigorous reaction conditions were needed. The as-prepared Pt NPs–MWNTs, which exhibited high catalytic efficiency, was used for amperometric sensing. With glucose oxi-

---

* Corresponding author at: State Key Laboratory of Electroanalytical Chemistry, Changchun Institute of Applied Chemistry, Chinese Academy of Sciences, Renming Street 5625, Changchun, Jilin 130022, PR China. Tel.: +86 431 85262101; fax: +86 431 85689711.
E-mail address: dongsj@ciac.jl.cn (S. Dong).

0039-9140/$ – see front matter © 2009 Elsevier B.V. All rights reserved.
doi:10.1016/j.talanta.2009.05.025

dase (GOD) as a model enzyme, a nanocomposite-based biosensor with fast and sensitive response was fabricated.

2. Experimental

2.1. Reagents and materials

GOD (EC 1.1.3.4, type II-S, 35600 U/g from *Aspergillus niger*) was obtained from Sigma Chemical Co. and used as received. MWNTs (80% purity, diameter 20–50 nm) purchased from Shenzhen Nanotech. Port. Co. Ltd. (Shenzhen, China) were purified through a well-established method with slight modification [22]. Nafion solution (0.5 wt%) was prepared by dilution of 5% Nafion solution (Aldrich) with alcohol. A 30% H_2O_2 solution was purchased from Beijing Chemical Reagent (Beijing, China) and a fresh solution of H_2O_2 was prepared daily. β-D-(+)-Glucose was also purchased from Beijing Chemical Reagent (Beijing, China) and the stock solution was allowed to mutarotate at room temperature overnight before use. Other chemicals were of analytical grade. Double distilled water was used throughout. A 0.1 M phosphate buffer solution (PBS) (pH 7.1) consisting of KH_2PO_4 and Na_2HPO_4 was employed as the supporting electrolyte.

2.2. Preparation of Pt NPs–MWNTs

To deposit Pt NPs onto the functionalized MWNTs, 1 mg of MWNTs was dispersed in 10 mL water by ultrasonic vibration for 0.5 h. Then 0.5 mL of 1% H_2PtCl_6 was added to the CNTs suspension with continuous stirring. Excess reducing agent, 1.5 mL $NaBH_4$ (0.1 M) was added to the mixture for the complete reduction of H_2PtCl_6 (stirring is necessary throughout the whole process). The resulted product was purified by centrifugation. After washing with water for 3 times, the black precipitation was redispersed into 2 mL water.

2.3. Preparation of modified electrode

Glassy carbon (GC, 2.6 mm in diameter) electrode was polished with 1.0 and 0.3 μm alumina slurry sequentially and then washed ultrasonically in water and ethanol for a few minutes, respectively. The cleaned GC electrode was dried with a high-purify nitrogen steam for the next modification. 3 μL of Pt NPs–MWNTs was spread evenly onto the GC electrode surface twice, and the electrode was dried to evaporate the solvent. Then 5 μL of GOD solution (2, 4, 6.7, 10 or 20 mg/mL, i.e. 0.36, 0.71, 1.19, 1.78 or 3.56 U) was dropped onto the Pt NPs–MWNTs modified electrode. After the film was dried, 5 μL of Nafion (0.5 wt.%) was coated on the electrode to form a thin layer. This modified electrode was called Nafion/GOD/Pt NPs–MWNTs/GC electrode. The Nafion/Pt NPs–MWNTs/GC or Nafion/GOD/GC electrode was prepared by spreading 6 μL of Pt NPs–MWNTs or 5 μL of GOD onto the GC electrode, and then coated with Nafion. The modified electrodes were stored at 4 °C under dry condition in a refrigerator if not used.

2.4. Apparatus and measurements

The transmission electron microscopy (TEM) images were recorded using a Hitachi H-8100 transmission electron microscope operated at 200 kV. The inductively coupled plasma-mass spectrometry (ICP-MS, Xseries^{II}, Thermo Scientific, USA) was used to determine the Pt content in Pt NPs–MWNTs nanocomposite. The X-ray photoelectron spectroscopy (XPS) was carried out on an ESCALAB-MKII spectrometer (VG Co.) with Al KR X-ray radiation as the X-ray source for excitation. UV–vis detection was performed on a Cray 50 UV–vis spectrophotometer (Varian, USA).

All electrochemical measurements were carried out at a CHI 832 electrochemical workstation (Shanghai, China). The modified electrode was used as the working electrode. Platinum flat and Ag/AgCl (saturated KCl) were used as the counter electrode and the reference electrode, respectively. Magnetic stirring was used mildly throughout amperometric measurements.

The electroactive surface area of the nanocomposite modified electrode was estimated according to the Randles–Sevcik equation [23] (measured for 9 times):

$$I_p = 2.69 \times 10^5 n^{3/2} A D^{1/2} \nu^{1/2} c \qquad (1)$$

where n, D, ν, and c are constant values, and A (cm^{-2}), the area of the electrode, is a linear function of the peak current of 5 mM Fe$(CN)_6{}^{3-}$.

3. Results and discussion

3.1. Preparation of Pt NPs–MWNTs

CNTs are very hydrophobic and cannot be wetted by liquids due to their high surface tension, thus, most metals would not adhere to them [24,25]. Surface modification and sensitization have been adopted attempting to improve metal deposition onto CNTs. One of the useful approaches is associated with the oxidation of the CNTs surface to create functional groups and increase metal nucleation [26,27]. In our strategy, the oxidative functional groups were introduced by the purification procedure of MWNTs with a mixture of HNO_3 and H_2SO_4 (1:3). The functional groups, such as carboxylic acid and hydroxide groups, attached to the outer surface of MWNTs could act as the anchor seeds for Pt NPs deposition [7]. UV–vis spectrophotometry was used to characterize the reduction of $PtCl_6{}^{2-}$. As is expected, there is a strong absorption band at 260 nm that corresponds to the absorption of $PtCl_6{}^{2-}$, while in the UV spectrum of Pt NPs–MWNTs the absorption peak disappears, indicating the successfully reduction of $PtCl_6{}^{2-}$ (data not shown). Furthermore, the ratio of Pt:MWNTs was determined to be 3:2 through ICP-MS.

3.2. TEM images

The morphologies and microstructures of the as-prepared nanocomposite were investigated using TEM. Fig. 1A displays the representative TEM images of Pt NPs–MWNTs. The dark spots and light tubes features correspond to Pt NPs and MWNTs, respectively. As can be seen, the side walls of MWNTs with diameters of 20–50 nm are covered with Pt NPs which are uniformly distributed, compared with MWNTs (Fig. 1B). The high-magnification images are shown in Fig. 1C and D to give more detailed information of Pt NPs supported on MWNTs; the fine Pt NPs are almost spherical. From the particle size distribution histogram (Fig. 1E), it was found that the Pt NPs mainly range from 10 to 30 nm and the average size of the as-prepared Pt nanostructure is about 22 ± 7 nm.

3.3. XPS spectrum

XPS measurements were also performed to identify and characterize the Pt NPs–MWNTs nanocomposite. As illustrated in Fig. 2, peaks at 71.1 and 74.4 eV correspond to Pt ($4f_{7/2}$) and Pt ($4f_{5/2}$), respectively, which are in good agreement with Pt (0) state [28] and further confirm the existence of Pt NPs on MWNTs.

3.4. Electrochemical characterization of Pt NPs–MWNTs

Cyclic voltammetry was employed to characterize the electrochemical behavior of Pt NPs supported on MWNTs in 0.2 M H_2SO_4 (Fig. S1). It is clear there are two pairs of peaks in the potential range

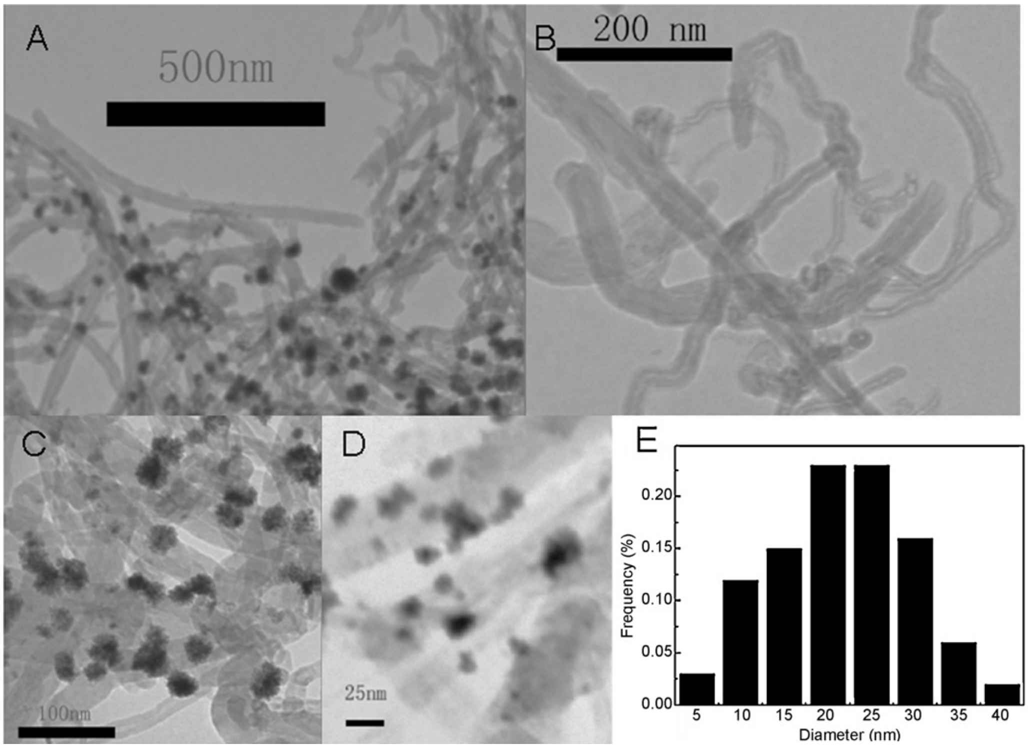

Fig. 1. TEM images of MWNTs and Pt NPs–MWNTs nanocomposite (A–D) and the particle size distribution histograms of Pt NPs (E).

from −0.20 to 0.10 V corresponding to the adsorption/desorption of hydrogen adatoms. The anodic oxidation starting at about 0.59 V is due to the formation of the platinum oxide that is subsequently reduced, as indicated by the appearance of a reduction peak at 0.46 V in the negative potential scan. The results exhibit the characteristic features expected for polycrystalline Pt [29,30]. In addition, during 50 successive scans, no observable peak current change was found implying that the Pt NPs–MWNTs immobilized with Nafion is stable.

3.5. Amperometric detection of H_2O_2

The cyclic voltammograms (CVs) measured using Pt NPs–MWNTs coated electrode in the absence (a) and presence (b) of 5 mM H_2O_2 in 0.1 M PBS (pH 7.1) are shown in Fig. 3A. It is observed that the Nafion/Pt NPs–MWNTs/GC electrode exhibits strong oxidation current starting at around 0.25 V. This substantially lowered the detection potential for H_2O_2 compared to the bulk glassy carbon electrode, which shows an oxidation of H_2O_2 starting at 0.8 V (data not shown). These results indicate that Pt NPs–MWNTs dramatically enhanced the oxidation of H_2O_2. Meanwhile, the scan rate controlled experiment shows the anodic currents at 0.7 V are linearly related with the square root of the scan in range from 10 to 200 mV/s, indicating a diffusion controlled process.

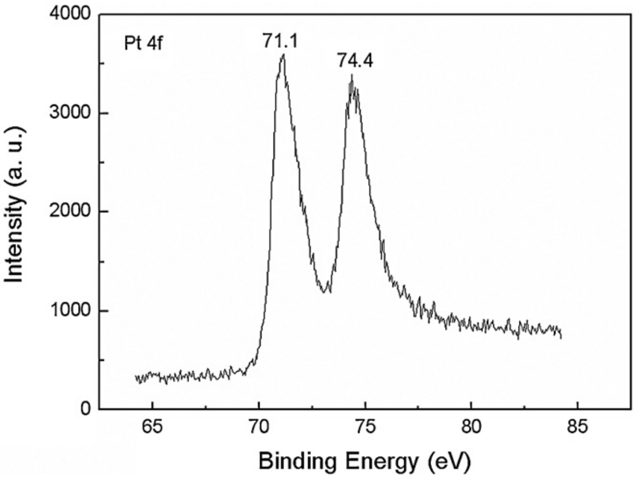

Fig. 2. XPS spectrum of Pt NPs–MWNTs.

Due to the prominent catalytic properties of CNTs and Pt NPs, Pt NPs–MWNTs facilitated amperometric detection of H_2O_2. The dependence of current response at the Nafion/Pt NPs–MWNTs/GC electrode on applied potential was studied and 0.7 V was chosen for the detection (Fig. S2). Fig. 4 shows the typical amperometric response recorded at the Nafion/Pt NPs–MWNTs/GC electrode by successive addition of H_2O_2 with an ascending order of concentration. That is 0.5, 0.5, 0.5, 1.0, 1.0, 1.0, 2.5, 2.5, 5.0, 5.0, 20, 20, 40, 40, 40, 40, 80, 80, 200, 200, 400, 400, 400, and 1000 μM, respectively. The nanocomposite-based electrode exhibits quick (within 3 s) and sensitive response with a wide linear range of 0.5 μM–2.9 mM and a detection limit of 0.1 μM based on S/N = 3. The sensitivity was calculated to be 591.33 $\mu A\,mM^{-1}\,cm^{-2}$ which is higher than other H_2O_2 sensors, such as 0.07 $\mu A\,mM^{-1}\,cm^{-2}$ at HRP/CNT electrode [31], 58.33 $\mu A\,mM^{-1}\,cm^{-2}$ at Nafion/Pt/CNT/GC electrode [32] and 260 $\mu A\,mM^{-1}\,cm^{-2}$ at PTNW–CNT–CHIT/GC electrode [33]. The high sensitivity and low detection limit obtained on the nanocomposite modified electrode should be not only attributed to the extra active surface provided by CNTs and Pt NPs, but also be explained by the synergistic action of CNTs and nanomaterials, which is widely supported by previous reports [34,35].

3.6. Performance of the Pt NPs–MWNTs-based glucose biosensor

The excellent performance of the nanocomposite modified electrode toward the detection of H_2O_2 makes it attractive for the fabrication of oxidase-based biosensors. GOD was selected as a

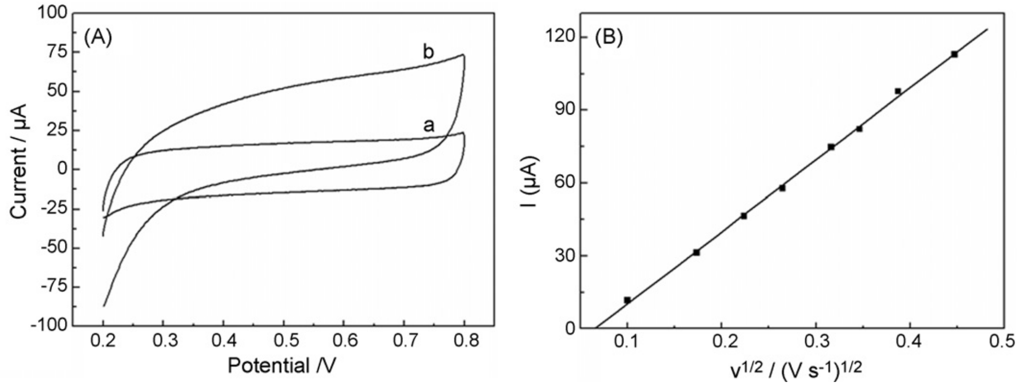

Fig. 3. (A) CVs of the Nafion/Pt NPs–MWNTs/GC electrode in the absence (a) and presence of 5 mM H_2O_2. The scan rate is 50 mV/s. (B) Diagram of I_p vs scan rate in range from 10 to 200 m V/s.

model enzyme and a glucose biosensor was constructed when GOD immobilized onto the Pt NPs–MWNTs/GC electrode surface using a thin layer of Nafion.

It is worth noting that the Nafion/GOD/Pt NPs–MWNTs/GC electrode (noted as electrode I) is sensitive toward glucose, whereas the other electrodes like Nafion/GOD/GC and Nafion/Pt NPs–MWNTs/GC electrodes (noted as electrodes II and III, respectively) exhibit negligible response (Fig. 5). This is because the glucose amperometric sensing of the three modified electrodes undergoes different approaches. For electrode II, electrons are generated through the following electrochemical reactions:

$$\text{glucose} + O_2 \xrightarrow{\text{GOD}} \text{gluconolactone} + H_2O_2 \qquad (2)$$

$$H_2O_2 \xrightarrow{\text{E}} H_2O + O_2 + 2e^- \qquad (3)$$

The slight current response can be ascribed to the oxidation of a small quantity of H_2O_2. As we known, the electro-oxidation of glucose could occur on a bare Pt electrode or mesoporous Pt [36,37] and a series of nonenzymatic glucose sensors based on platinum nanomaterials have been constructed by Xia and co-workers [38,39]. Herein, we think the electro-oxidation of glucose has taken place on Pt NPs–MWNTs to bring the current response of the electrode III. When electrode I was employed in glucose sensing, much higher sensitivity was obtained. The mechanism of the nanocomposite-based biosensor was proposed as follow: the electrochemical reaction firstly involves similarly to (2), however, the product, H_2O_2, which then undergoes oxidation on the nanocomposite with larger active surface area and higher electrocatalytic activity instead of GC electrode surface, releasing two electrons. The two electrons transfer from the nanocomposite to the electrode and result in the current signal. The presence of GOD and Pt NPs–MWNTs bring up a significant increased response, which could be mainly attributed to the high electrocatalytic activity toward H_2O_2 of Pt NPs–MWNTs we prepared. The result is in good agreement with that in Section 3.5.

The amount of enzyme immobilized on the nanocomposite matrix is an important parameter for the sensitivity, reproducibility, and stability of the biosensor [40]. Various GOD loading within the biosensor was studied, namely, 2, 4, 6.7, 10, and 20 mg/mL (0.36, 0.71, 1.19, 1.78 or 3.56 U). The performance of the biosensor containing different amounts of enzyme in glucose detection is illustrated in Table S1 (Supporting Information). It seems that low GOD content leads to a wider linear range; however, the amperometric response is improved by raising the concentration of GOD from 2 to 10 mg/mL. Higher GOD content, such as 20 mg/mL, results in an obvious decreased current response with the successive addition of glucose, which could be explained as follow. On one hand, at higher enzyme content, the electron-relaying capacity of the

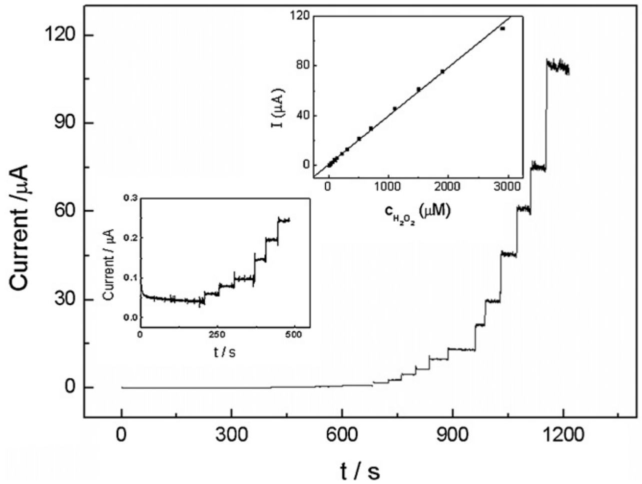

Fig. 4. Amperometric response for increasing H_2O_2 concentration obtained at the Nafion/Pt NPs–MWNTs/GC electrode in 0.1 M PBS (pH 7.1). Applied potential: 0.7 V (vs Ag/AgCl). The concentration of successive addition of H_2O_2 is 0.5, 0.5, 0.5, 1.0, 1.0, 1.0, 2.5, 2.5, 5.0, 5.0, 20, 20, 40, 40, 40, 40, 80, 80, 200, 200, 400, 400, 400, and 1000 μM, respectively. Inset (up) shows the calibration curve for H_2O_2 from 0.5 μM to 2.9 mM. Inset (down) shows magnification of response at 0.5, 0.5, 0.5, 1.0, 1.0, and 1.0 μM.

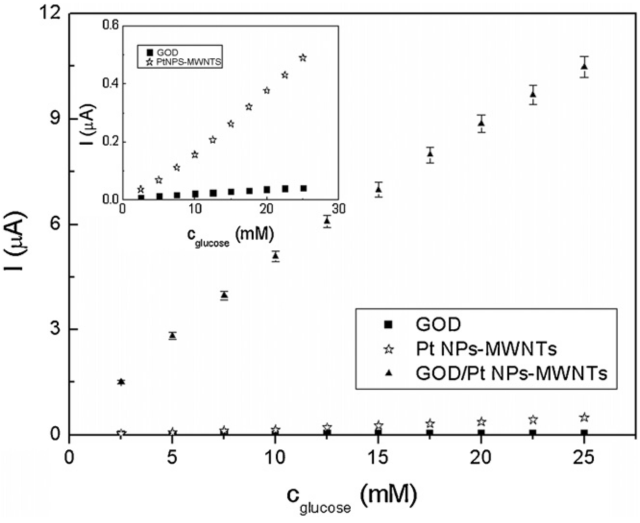

Fig. 5. Calibration curves for glucose obtained at the Nafion/GOD/GC (■), Nafion/Pt NPs–MWNTs/GC (☆), and Nafion/GOD/Pt NPs–MWNTs/GC (▲) electrodes in 0.1 M PBS (pH 7.1). Applied potential: 0.70 V (vs Ag/AgCl).

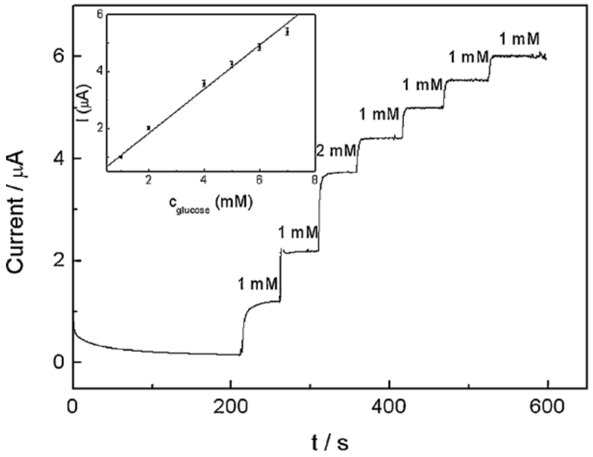

Fig. 6. Amperometric response for increasing concentration of glucose obtained at the Nafion/GOD/Pt NPs–MWNTs/GC electrode in 0.1 M PBS (pH 7.1). Applied potential: 0.70 V (vs Ag/AgCl). Inset shows the calibration curve of glucose obtained at the Nafion/GOD/Pt NPs–MWNTs/GC electrode.

GOD/nanocomposite film is diminished by the nonrelaying GOD in the network, which results the transport of electrons to the bound enzyme molecules not fast enough to match their turnover rate at a substrate concentration [41,42]. On the other hand, too high enzyme concentration would cause leakage of the enzyme from the modified electrode. In general, the amount of the GOD on the nanocomposite does not significantly affect the performance of the biosensors, which might be due to the high electrocatalytic activity of Pt NPs–MWNTs.

Fig. 6 displays the typical amperometric response of the Nafion/GOD/Pt NPs–MWNTs/GC electrode with the GOD loading of 10 mg/mL for the successive addition of glucose at 0.7 V in the stirred PBS (pH 7.1). The calibration curve (inset) for the glucose biosensor under optimal experimental conditions shows a linear response to glucose concentration in the range of 1–7 mM with a detection limit of 3 μM and a response time of 3 s, respectively. The detection limit of our materials is indeed lower than some kind of biosensor based on the Pt/CNTs hybrids (e.g., 0.4 mM at GOD/Aunano/Ptnano/CNT electrode [43] and 8.89 μM at biosensors based on Pt NPs–ACNTs [44]). It is also superior to a highly ordered carbon (OMC)-based glucose biosensor (156.52 μM) [45] and an optical biosensor based on nanocomposite films of CdTe quantum dots and GOD (0.5 mM) [46].

The biosensor with GOD concentration of 10 mg/mL showed the catalytic current response maintained 96% of its initial value in one week (used daily) and 81% after two months. The presence of Nafion avoids the leakage of enzyme as well as nanocomposite and also serves as an effective permselective barrier to electroactive interferences frequently found in actual samples. There were no observable response obtained at the Nafion/GOD/Pt NPs–MWNTs/GC electrode by addition of 0.1 mM ascorbic and uric acid.

4. Conclusions

A facile and simple "one-pot" route has been demonstrated for the preparation of the Pt NPs–MWNTs nanocomposite, where any other stabilizing agents were not required. Electrochemical results revealed the nanocomposite exhibited high electrocatalytic activity toward the oxidation of H_2O_2. Thus, with GOD as a model enzyme, an oxidase-based glucose biosensor with a high sensitivity and low detection limit was constructed. Additionally, we discussed the respective roles of Pt NPs–MWNTs and GOD in the glucose amperometric sensing.

Acknowledgments

The work was supported by the National Natural Science Foundation of China (Nos. 20675076 and 20820102037).

Appendix A. Supplementary data

Supplementary data associated with this article can be found, in the online version, at doi:10.1016/j.talanta.2009.05.025.

References

[1] S.J. Guo, S.J. Dong, Trends Anal. Chem. 28 (2009) 96.
[2] K. Makino, K. Furukawa, K. Kajima, J. Power Sources 166 (2007) 30.
[3] G. Chang, M. Oyama, K. Hirao, J. Phys. Chem. B 110 (2006) 1860.
[4] S.A.G. Evans, J.M. Elloit, L.M. Andrews, P.N. Barlett, P.J. Doyle, G. Denuault, Anal. Chem. 74 (2002) 1322.
[5] L.H. Xu, Y.H. Zhu, L.H. Tang, C.Z. Li, Electroanalysis 19 (2007) 717.
[6] J. Lu, I. Do, L.T. Drzal, R.M. Worden, I. Lee, ACS Nano 2 (2008) 1825.
[7] J.N. Xie, S. Wang, L. Aryasomayajula, V.K. Varadan, Nanotechnology 18 (2007) 65503.
[8] Y. Ikariyama, S. Yamauchi, T. Yukiashi, H. Ushioda, Anal. Lett. 20 (1987) 1791.
[9] H. Dai, Acc. Chem. Res. 35 (2002) 1035.
[10] J.J. Niu, J.N. Wang, Electrochim. Acta 53 (2008) 8058.
[11] D.J. Guo, H.L. Li, J. Electroanal. Chem. 573 (2004) 197.
[12] J. Wang, Y.H. Lin, Trends Anal. Chem. 27 (2008) 619.
[13] S. Hrapovic, Y. Liu, K.B. Male, J.H.T. Luong, Anal. Chem. 76 (2004) 1083.
[14] K.B. Male, S. Hrapovic, J.H.T. Luong, Analyst 132 (2007) 1254.
[15] M. Yang, Y. Yang, Y. Liu, G. Shen, R. Yu, Biosens. Bioelectron. 21 (2006) 1125.
[16] Y.C. Tsai, S.Y. Chen, C.A. Lee, Sens. Actuators B 135 (2008) 96.
[17] G. Girishkumar, K. Vinodgopal, P.V. Kamat, J. Phys. Chem. B 108 (2004) 19960.
[18] P. Serp, M. Corrias, P. Kalck, Appl. Catal. A: Gen. 253 (2003) 337.
[19] J.V. Zoval, J. Lee, S. Gorer, R.M. Penner, J. Phys. Chem. B 102 (1998) 1166.
[20] H.C. Choi, M. Shim, S. Bangsaruntip, H. Dai, J. Am. Chem. Soc. 124 (2002) 9058.
[21] M. Musameh, N.S. Lawrence, J. Wang, Electrochem. Commun. 7 (2005) 14.
[22] J. Liu, A.G. Rinzler, H.J. Dai, J.H. Hafner, R.K. Bradley, P.J. Boul, L. Adrian, T. Iverson, K. Shelimov, C.B. Huffman, F. Rodriguez-Macias, S. Young-Seok, T.R. Lee, D.T. Colbert, R.E. Smalley, Science 280 (1998) 1253.
[23] A.J. Bard, L.R. Faulkner, Electrochemical Methods: Fundamentals and Applications, Wiley, New York, 2001, pp. 228–234.
[24] E. Dujardin, T.W. Ebbesen, H. Hiura, K. Tanigaki, Science 265 (1994) 1850.
[25] V. Lordi, N. Yao, J. Wei, Chem. Mater. 13 (2001) 733.
[26] Y.P. Sun, K. Fu, Y. Lin, W. Huang, Acc. Chem. Res. 35 (2002) 1096.
[27] T.W. Ebbesen, H. Hiura, M.E. Bischer, Adv. Mater. 8 (1996) 155.
[28] E. Drawdy, G.B. Hoflund, S.D. Gardner, E. Yngvadottir, D.R. Schryer, Surf. Interface Anal. 16 (1990) 369.
[29] J. Chou, S. Jayaraman, A.D. Ranasinghe, E.W. McFarland, S.K. Buratto, H. Metiu, J. Phys. Chem. B 110 (2006) 7119.
[30] A. Kicela, S. Daniele, Talanta 68 (2006) 1632.
[31] L. Qian, X.R. Yang, Talanta 68 (2006) 721.
[32] H. Tang, J.H. Chen, S.Z. Yao, L.H. Nie, G.H. Deng, Y.F. Kuang, Anal. Biochem. 331 (2004) 89.
[33] F.L. Qu, M.H. Yang, G.L. Shen, R.Q. Yu, Biosens. Bioelectron. 22 (2007) 1749.
[34] J. Li, J.D. Qiu, J.J. Xu, H.Y. Chen, X.H. Xia, Adv. Funct. Mater. 17 (2007) 1574.
[35] M.H. Yang, Y. Yang, H.F. Yang, G.L. Shen, R.Q. Yu, Biomaterials 27 (2006) 246.
[36] Y.B. Vassilyev, O.A. Khazova, N.N. Nikolaeva, J. Electroanal. Chem. 196 (1985) 105.
[37] S. Park, T.D. Chung, H.C. Kim, Anal. Chem. 75 (2003) 3046.
[38] L.Q. Rong, C. Yang, Q.Y. Qian, X.H. Xia, Talanta 72 (2007) 819.
[39] J.H. Yuan, K. Wang, X.H. Xia, Adv. Funct. Mater. 15 (2005) 803.
[40] Y.C. Tsai, S.C. Li, J.M. Chen, Langmuir 21 (2005) 3653.
[41] M. Vreeke, R. Maidan, A. Heller, Anal. Chem. 17 (1992) 921.
[42] M. Elmgren, S.E. Lindquist, M.J. Sharp, Electroanal. Chem. 64 (1992) 3084.
[43] X. Chu, D.X. Duan, G.L. Shen, R.Q. Yu, Talanta 71 (2007) 2040.
[44] K. Zhao, S.Q. Zhuang, Z. Chang, H.Y. Songm, L.M. Dai, P.G. He, Y.Z. Fang, Electroanalysis 19 (2007) 1069.
[45] M. Zhou, L. Shang, B.L. Li, L.J. Huang, Biosens. Bioelectron. 24 (2008) 442.
[46] X.Y. Li, Y.L. Zhou, Z.Z. Zheng, X.L. Yue, Z.F. Dai, S.Q. Liu, Z.Y. Tang, Langmuir 25 (2009) 6580.